Gümüşhane University Journal of Science

GUFBD / *GUJS* (2024) 14(2): 526-537 doi: 10.17714/gumusfenbil.1269155 Research Article

Potential controlled electrochemical coating and characterization of nanocrystalline Sn-Zn based thin films

Nanokristal Sn-Zn bazlı ince filmlerinin gerilim kontrollü elektrokimyasal kaplanması ve karakterizasyonu

Begüm ÜNVEROĞLU ABDİOĞLU*

Ankara Yıldırım Beyazıt University, Faculty of Engineering and Natural Sciences, Department of Metallurgy and Materials Engineering, 06010, Ankara

• Received: 22.03.2023 • Accepted: 07.02.2024

Abstract

Sn-Zn thin films are commonly used in many areas of the industry, and the facile production of these layers is vital. This study aims to produce Sn-Zn layers via potentially controlled electrochemically deposited coatings. The potentially controlled mode was used to eliminate the extensive hydrogen evolution reaction during the electrochemical processes. The electrochemical reduction and oxidation reactions were first investigated with cyclic voltammetry to determine the applied potential sets. Later, cathodic pulse potential electrodeposition of the layers was performed. The characterization of the coated Sn-Zn thin films was performed with an X-ray diffraction device (XRD), scanning electron microscope (SEM), energy dispersive spectroscopy (EDS), four-point probe, potentiodynamic polarization measurements, and electrochemical impedance spectrometry. As the cathodic pulse potential value increased, the ratio of Zn in the Sn-Zn alloy increased, and the microstructure of the layers was also affected. Electrochemical studies showed that the corrosion resistance of the Sn-Zn thin films increased with the increasing Zn amount in the coating.

Keywords: Corrosion resistance, Electrochemical coating, Pulse potential, Sn-Zn alloy

Öz

Sn-Zn ince filmler endüstrinin birçok alanında yaygın olarak kullanılmaktadır ve bu katmanların kolay üretimi önem taşımaktadır. Bu çalışma, potansiyel olarak kontrollü elektrokimyasal olarak biriktirilmiş kaplamalar yoluyla Sn-Zn katmanları üretmeyi amaçlamaktadır. Potansiyel olarak kontrol edilen mod, elektrokimyasal işlemler sırasında şiddetli hidrojen oluşumu reaksiyonunu ortadan kaldırmak için kullanılmıştır. İlk olarak, elektrokimyasal indirgeme ve oksidasyon reaksiyonları, uygulanan potansiyel setlerini belirlemek için döngüsel voltametri ile araştırılmıştır. Daha sonra katmanların katodik darbe potansiyelli elektrokaplaması gerçekleştirilmiştir. Kaplanmış Sn-Zn ince filmlerin karakterizasyonu X-ışını kırınım cihazı (XRD), taramalı elektron mikroskobu (SEM), enerji dağılımlı spektroskopi (EDS), dört noktalı prob, potansiyodinamik polarizasyon ölçümleri ve elektrokimyasal empedans spektrometrisi ile gerçekleştirilmiştir. Katodik darbe potansiyeli değeri arttıkça Sn-Zn alaşımındaki Zn oranı artmış ve katmanların mikro yapısı da etkilenmiştir. Elektrokimyasal çalışmalar, Sn-Zn ince filmlerinin korozyon direncinin, kaplamadaki Zn miktarının artmasıyla arttığını göstermiştir.

***Anahtar kelimeler**: Korozyon direnci, Elektrokimyasal kaplama, Darbeli potansiyel, Sn-Zn alaşımı*

*Begüm ÜNVEROĞLU ABDİOĞLU; bunveroglu@aybu.edu.tr

1. Introduction

Binary alloy coatings in the industry have always been vital to obtain mechanical stability, corrosion protection, and the aesthetic appearance of objects (Zangari, 2015). Besides, the industry needs a green solution for a sustainable production process (Baines et al., 2012). Some of the industrial alloys need replacement due to their toxic nature like Cd-based coatings (Zhirnov et al., 2003). Therefore, attempts to create alternative coatings with electrochemical baths without toxic electrolytes such as cyanide are the center of attraction of binary and ternary alloy electrodeposition systems. The Sn-Zn binary alloys have the potential to replace some of the toxic elements like Cd and Pb in various applications. Sn-Zn thin film coatings can be used as a solder material, as a glucose sensor, as a corrosion protection layer, and as a lubricant layer (Hou et al., 2019; Khan et al., 2020; Pereira et al., 2012; Yamada & Usami, 2022).

Sn-Zn alloy electrodeposited were reported in the literature, for different baths with various additives, pH values, and complexing agents (Esfahani et al., 2018; Hairin et al., 2018; Pereira et al., 2012). The first Sn-Zn films were electrodeposited from cyanide-based solutions but, alternative baths were reported in the literature (Hairin et al., 2018; Kazimierczak et al., 2014; Kazimierczak & Ozga, 2013; Taguchi et al., 2008). However, more environmentally friendly electrolyte alternatives are required in our era. In a recent study, an environmentally friendly approach was reported in the literature with a citrate-based electrolyte. Kazimierczak et al (2014) studied the electrodeposition behavior of Zn-Sn citrate baths with cyclic voltammetry and stability tests (Kazimierczak et al., 2014). In their studies, they found that the stability and existence of metal ions are strongly dependent on the solution pH. They used a complexing agent, trisodium citrate, to narrow the electrodeposition window of the Zn-Sn system and indicated that in the pH range of 4.5-6 citrate-tin and citrate-zinc coexist together. The current efficiency of the system is reported to stay around 85-90% at more negative potentials than -1.0 V.

Although citrate-based baths are environmentally friendly and do not require toxic additives, the presence of hydrogen evolution reaction (HER) is a bottleneck to obtaining smooth, uniform, and high-quality coatings (Munir et al., 2018; Tsurusaki & Ohgai, 2020). Because, a continuous hydrogen evolution reaction causes local pH change, resulting in the generation of fragile Zn compounds through the consumption of $ZnSO_4$ electrolyte and active Zn metal, all these cause unevenness of the electrode surface (Zhai et al., 2022). Besides that, the regions with a strong electric field, where hydrogen evolution reactions take place accelerate vertical dendrite growth rather than planer growth of Zn (Zhai et al., 2022).

To overcome these negative effects of Zn electrodeposition, various strategies have been proposed to suppress the Zn dendrite growth such as surface modification of the working electrode, changing electrodeposition parameters, or modifying electrolyte recipe (Choi et al., 2006; Pereira et al., 2012; Taguchi et al., 2008). Depending on the deposition parameters coatings with different compositions and morphologies can be obtained (Jung et al., 2009; Kazimierczak et al., 2014; Khan et al., 2020). Applied potential is an important parameter not only for composition but also for physical properties of the coating such as roughness, thickness, and morphology of the layers due to the co-existent reaction, hydrogen evolution, in Zn electrodeposition. Therefore, controlling the applied potential to produce homogenous Sn-Zn alloys is one way to modify the quality of the layers. So far, the various researchers put efforts to manufacture anticorrosive Sn-Zn layers for different applications with alternative electrolytes and deposition parameters, and their endeavors collected around understanding the electrolyte and electrodeposition system, however, only a limited number of researchers have reported the electrodeposited layers' electrochemical behavior along with the chemical, structural and morphological behaviors (Alesary et al., 2020; Benidir et al., 2022; Choi et al., 2006; Fashu et al., 2015; Hadi Wijaya & Soegijono, 2019; Pereira et al., 2021).

This study aims to coat Sn-Zn layers from a citrate-based electrolyte with a cathodic pulsed potential electrodeposition mode to minimize the harmful effects of hydrogen evolution reaction. Understanding the deposition behavior of the Sn-Zn electrolyte is crucial for defining the precise deposition potentials, therefore, various characterization techniques were applied to investigate the influences of applied potential sets on the layer properties in this study.

2. Material and method

A typical three-electrode cell was used to electrodeposit Sn-Zn thin film from a simple solution. The carbon was used as a counter electrode, Ag/AgCl was used as a reference electrode, and 316 SS steel foil was used as a working electrode. The 316 SS steel foil substrate is mechanically polished with sandpapers (320-1200), cleaned with ethanol, etched in dilute H_2SO_4, and rinsed in distilled water before each electrochemical deposition. The electrodeposition electrolyte contains 0.25 M $Na_3C_6H_5O_7$ as a supporting electrolyte, 104 mM $NaC_{12}H_{25}SO_4$ as complexing agents and a surfactant and metal salts. The metal salts 10 mM $ZnSO_4.7H_2O$, and 5 mM $SnSO_4$ were added to the electrolyte, respectively. All chemicals are analytical grade. The pH of the electrolyte was adjusted to 5.5 with a dilute H_2SO_4 and fresh electrolyte was used before each experiment. Cyclic voltammetry was applied with the scan rate of 25 mV/s between 0.5 V to -1.5 V to investigate the reduction-oxidation behavior of the electrolyte system. The cathodic pulse potential electrodeposition took place according to the parameters given in Table 1 at 20±2 °C for an hour each. These parameters were determined after cyclic voltammetry analyses.

Table 1. Cathodic pulse potential electrodeposition parameters

Sample Code	Pulse-on potential (V)	Pulse-reversal Potential (V)	Pulse-on Period (s)	Pulse-reversal Period (s)
-1.0V/-1.3V	-1.3	-1.0	30	30
-1.1V/-1.4V	-1.4	-1.1	30	30
-1.2V/-1.5V	-1.5	-1.2	30	30

The characterization of the Sn-Zn thin films was performed with the XRD analyses (Rigaku-Miniflex 600) where the structure was measured with CuKα radiation of 40 kV and 15 mA at a 2°/min scan rate. The average crystal size of the samples can be calculated according to the Debye-Scherrer formula given below.

$$D = \frac{0.94\,\lambda}{\beta \cos\theta} \tag{1}$$

Here D is the average crystal size of the samples, λ is the wavelength radiation, β is the FWHM of the selected X-ray diffraction peak and Θ is the diffraction angle. Besides that, the dislocation density and the crystal density are also important crystal parameters which influences physical and chemical properties of materials. Therefore, these parameters were also investigated according to the equations given below.

$$\delta = \frac{1}{D^2} \tag{2}$$

$$N = \frac{t}{D^3} \tag{3}$$

Here, δ is the dislocation density, N is the number of crystals per unit area and t is the thickness of the thin film. The SEM analyses were conducted with Hitachi SU 500 FE-SEM, the EDS analyses were performed with Oxford X- MaxN80. The four-point probe technique was used to determine the electrical resistivity with Lucas Labs Pro 4-Point Probe test system with Keithley 2400 standard series source and a TEKTRONIX Keithley Kickstart 2.0 software. The tungsten carbide tips with 1.016 mm tip spacing were used during the electrical measurements. Besides that, the following model for the four-point probe sheet resistance measurements was used for the thin film coatings.

$$R_{sh} = \frac{V}{I}\frac{\pi}{ln2} = \frac{V}{I}4.5324 \tag{4}$$

Here R_{sh} is the sheet resistance, V is the voltage between the inner probes, and I is the current through the outer probes. Besides that, the specific resistance of the thin films was calculated according to the formula given in equation 5. Here ρ and τ show the specific resistance and film thickness, respectively.

$$\rho = R_{sh}\tau \tag{5}$$

Current-voltage values of the films are calculated according to formula given below.

$$\rho = \frac{\pi t}{ln2}\left(\frac{V}{I}\right) \quad (6)$$

The corrosion behavior of samples was determined with potentiodynamic polarization curves in 3.5 wt% NaCl solution with a 5 mV/s scan rate and the electrochemical impedance spectrometry were investigated in 3.5 wt% NaCl solution with an amplitude of 5 mV between 1 Hz and 1 x 10^5 Hz. All the electrochemical experiments were performed with CH Instrument device.

3. Results and discussion

3.1. Cyclic voltammetry of Sn-Zn electrolyte system

The cyclic voltammetry curves for the Sn-Zn system have been shown in Figure 1. The cyclic voltammetry studies were held to understand the reduction and oxidation behaviour of the Sn-Zn electrolyte system. For that reason, cyclic voltammetry of the base solution (consisting of supporting electrolyte and the complexing agent), Sn electrolyte, Zn electrolyte and Sn-Zn electrolyte were investigated. A major cathodic peak and 5 anodic peaks were observed in the measurements. The large cathodic peak at around -1.2 V was corresponding to complexing agents and metal ion(s) in the electrolyte. In the literature, the cyclic voltammetry study of Sn and Zn metal ions in different electrolyte were reported for individual baths and alloy solution (Munir et al., 2018). It has been reported that the Zn ion reduction from Sn-Zn electrolyte was taking place at more positive potentials compared to Zn only electrolyte suggesting an earlier electrodeposition of Zn ions. In this study, the reduction is also taking place at slightly more positive potentials in the alloy electrolyte compared to Zn only electrolyte like the reported literature values. Besides that, the intensity of the peak was the lowest for the Sn-Zn electrolyte suggesting less HER in the binary electrolyte. The black curve was corresponding to base solution, and no specific anodic peaks were observed for this electrolyte. The anodic peaks A_1, A_2, and A_3 were attributed to the Sn and Sn complex dissolution. The peaks labelled as A_4 and A_5 were attributed to the Zn dissolution.

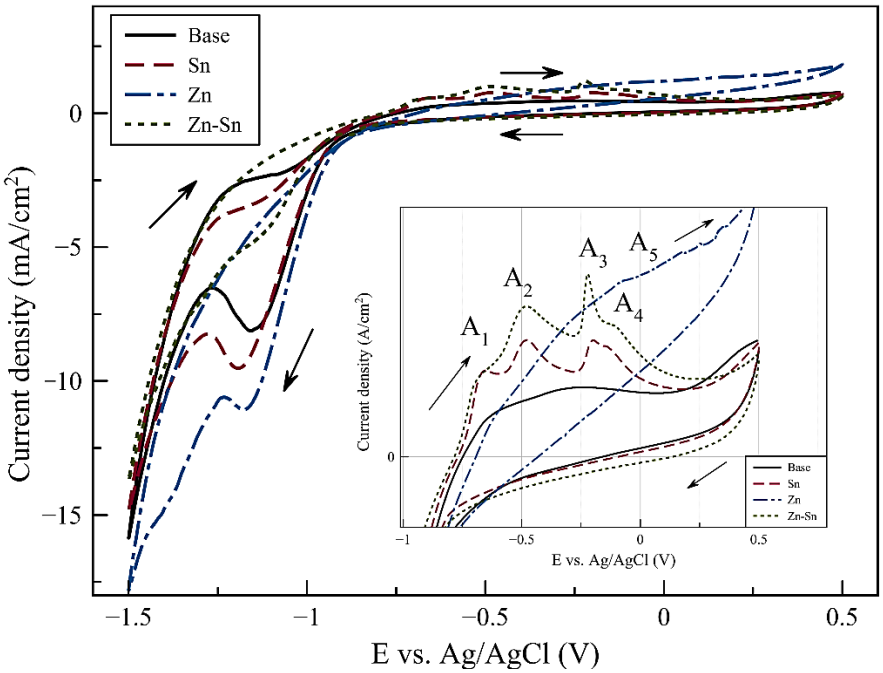

Figure 1. Cyclic voltammetry curves of Sn-Zn system, inset: the anodic region

3.2. Cathodic pulse potential electrodeposition of Sn-Zn thin films

The cathodic pulse potential electrodeposition was held with three different conditions. Figure 2 shows the current density and time graph for these samples during the first 400 seconds of the electrodeposition. First

more positive potential values were applied to the samples and then more negative potentials were applied to samples to start nucleation with low overpotentials. The current density for more negative potentials was higher compared to more positive potentials. Particularly, a dramatic increase in the current density was observed for the applied potential -1.5 V for the last sample due to the co-existing of high intensity HER and Zn reduction. The thickness of the layers has been found to be 32, 37 and 44 µm for -1.0/-1.3 V, -1.1/-1.4 V and -1.2/-1.5 V samples respectively according to SEM measurements.

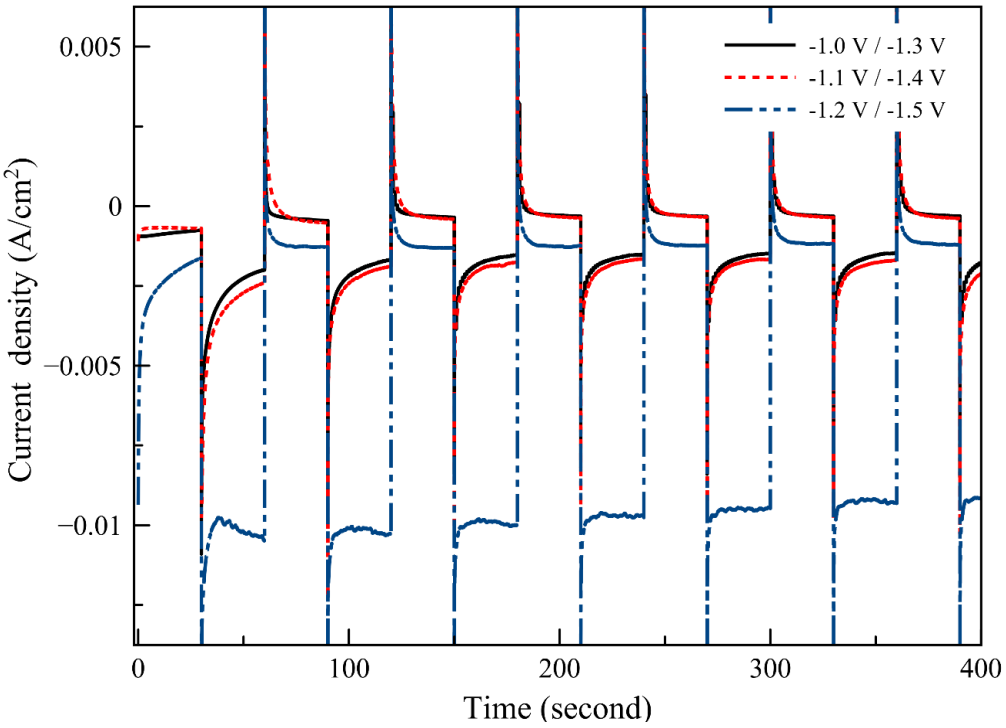

Figure 2. Current density and time graph for Sn-Zn thin film cathodic pulse potential set

3.3. Crystal Structure Analyses of Sn-Zn thin films

Figure 3 shows the XRD patterns for the Sn-Zn based thin films electrodeposited at different cathodic pulse potential conditions. In all layers, elemental Sn and Zn phases were observed with the tetragonal crystal structure of β-Sn and the hexagonal close-packed (HCP) crystal structure of the Zn phase according to standard data files (JCPDS number 01-089-2958 for Sn and JCPDS number 00-004-0784 for Zn). Besides Sn and Zn based phases, the coatings also contained oxide form of tin. One peak for the SnO_2 phase was observed in the XRD patterns according to the standard data file (JCPDS number 01-077-0447) which may come from the solution or formed during the electrodeposition process. The formation of Sn-Zn based thin films was investigated in the literature for different manufacturing systems. In the literature, the Sn-Zn thin films were also electrodeposited from a citrate-based electrolyte with a direct current and the hexagonal Zn phase and tetragonal β-Sn phase were also observed in their study (Salhi et al., 2016). In the literature study, only elemental phases of Sn and Zn were reported (Salhi et al., 2016). However, SnO_2 phase was not reported in the reported study in the literature (Salhi et al., 2016). The difference between the studies could be related to the electrodeposition mode change such as potentially controlled mode. The average crystal size of the samples was calculated according to the Debye Scherrer formula based on the most intense Sn and Zn peaks. The average crystal size of the samples according to Sn peak was 46 nm, 31 nm, and 33 nm for the samples electrodeposited with -1.0V/-1.3V, -1.1V/-1.4V, and -1.2V/-1.5V cathodic pulse potential conditions, respectively. The average crystal size of the samples according to Zn peak was 26 nm, 30 nm, and 33 nm for the samples electrodeposited with -1.0V/-1.3V, -1.1V/-1.4V, and -1.2V/-1.5V cathodic pulse potential conditions, respectively. The average crystal size of the Sn phases decreased slightly with the increasing applied negative potential set, whereas the average crystal size of the Zn phase increased slightly with the increasing applied negative potential sets. As the applied negative potential increases, the overpotential for the reduction of Zn metal ions increases which elevates the growth of the Zn crystals in the competitive Sn and

Zn reduction system. Therefore, it is possible that the Sn reduction was slightly suppressed under the competitive reactions and the crystal size of the Sn phase might have been influenced and resulted in slightly smaller average crystal sizes. The dislocation density and the crystallization density were calculated according to the main phase, Sn, and the results are listed in Table 2. The dislocation density slightly increased with the applied negative potential sets and the crystal density increased with the applied negative potential sets.

Table 2. Average crystal size, dislocation density and crystal density

Sample	Sn phase D (nm)	Zn phase D (nm)	δ (lines/nm^2)	N (1/nm^2)
-1.0V/-1.3V	46	26	0.000473	2.46 X 10^{-8}
-1.1V/-1.4V	31	30	0.001041	1.10 X 10^{-7}
-1.2V/-1.5V	33	33	0.000918	1.16 X 10^{-7}

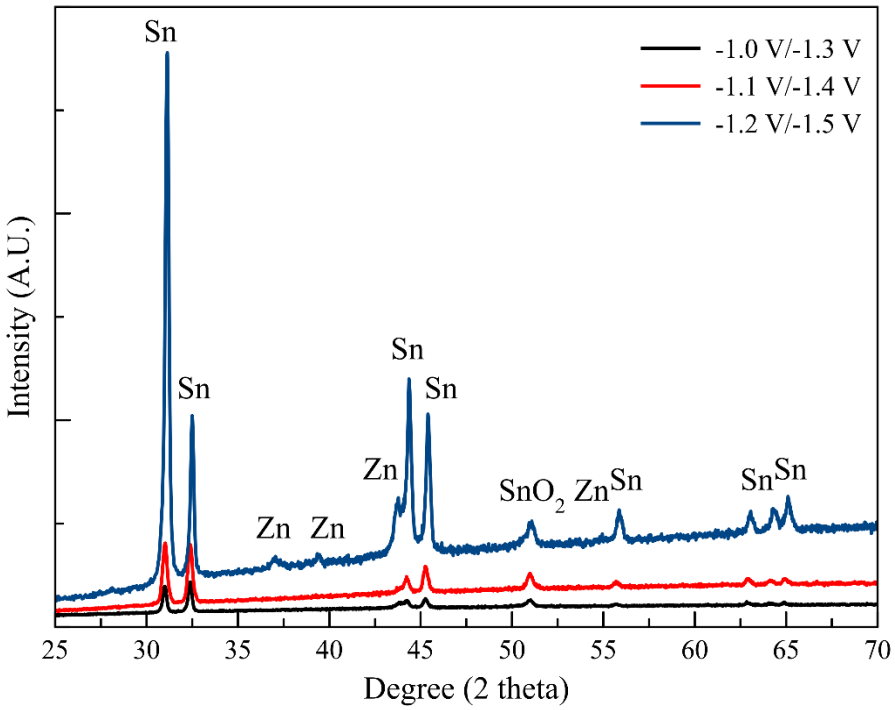

Figure 3. XRD analysis of Sn-Zn thin films

3.4. Compositional and morphological analyses of Sn-Zn thin films

The compositional fraction of the Sn-Zn thin films was measured and given in Table 3 with the standard deviations for elemental Sn and Zn. It has been found that the Zn at% was increased with the increasing applied overpotential sets. Besides that, the standard deviation of the Sn and Zn compositional fraction was increased with the applied overpotential sets.

Table 3. EDS elemental analysis of Sn-Zn thin films

Sample	Sn	Zn
-1.0V/-1.3V	96 at% ±0.9	4 at% ±1,5
-1.1V/-1.4V	91 at% ±1,2	9 at% ±1,8
-1.2V/-1.5V	60 at% ±1,4	40 at% ±2,1

Figure 4 shows the EDS element mapping of the Sn-Zn thin film which was electrodeposited with -1.1 V/-1.4 V cathodic pulse potential, together with a single element color map for the Sn and Zn individually. According to these figures, it can be said that the elements are homogeneously distributed over the substrate for both elements.

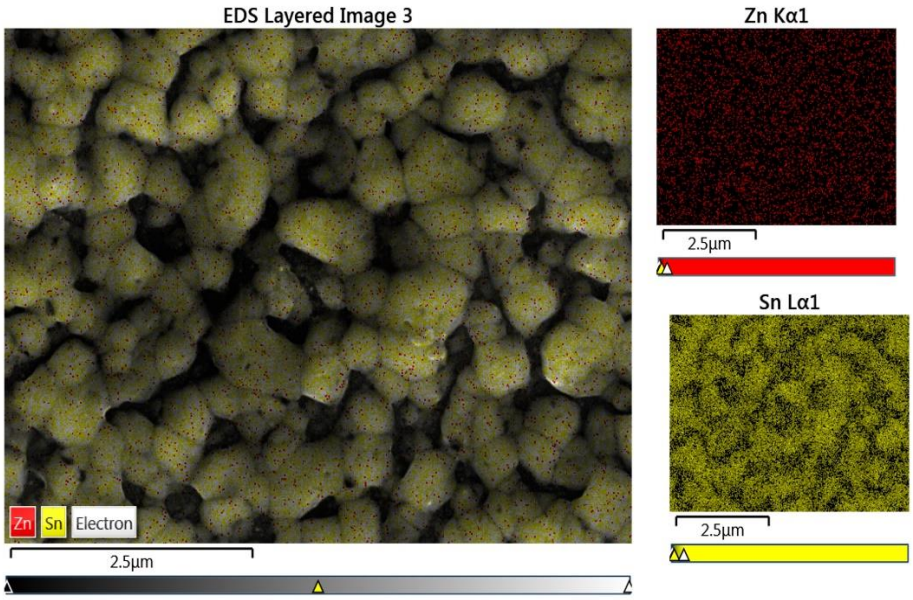

Figure 4. EDS element mapping of Sn-Zn thin film (-1.1V/ -1.4V)

Figure 5 shows the top-down SEM images of the electrodeposited Sn-Zn thin films. The surface of the substrate was covered mostly with the Sn-Zn layer without any macrogaps. The increasing overpotential of the cathodic pulse potential influenced on the morphology of the Sn-Zn thin films. In the first sample, Figure 5.(a), there exists an almost compact layer without large gaps. In the second sample, Figure 5.(b), the geometrically different formations began to form locally. In the last sample, Figure 5.(c), some features were distributed over the substrate and there exist microcracks through the layer. Please note that the composition of the layers is different, particularly for the last sample, therefore, the SEM images of the sample shows fundamental differences. In the literature, the morphology of Zn-Sn thin films and Sn-Zn thin films were reported for gluconate based and citrate-based electrolytes respectively (Esfahani et al., 2018; Kazimierczak et al., 2014). The reported morphology of Zn-Sn thin films electrodeposited with a pulse electrodeposition mode from a gluconate-based electrolyte was micron sized grains with gaps and rough surface (Esfahani et al., 2018). On the other hand, the reported morphology of Sn-Zn thin films electrodeposited with galvanostatic mode from a citrate-based electrolyte were micron sized and homogenous coatings (Kazimierczak et al., 2014). In this study, cathodic pulse potential was used to produce Sn-Zn layers from a citrate-based electrolyte and similar morphologies but with some microgaps and microcracks were observed different than the literature.

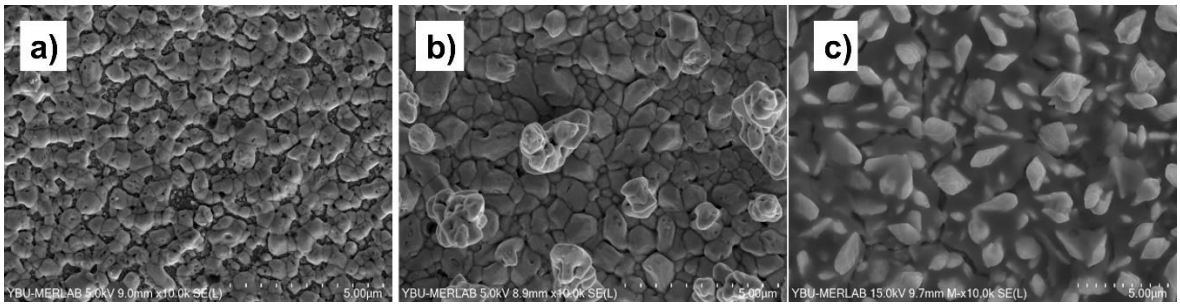

Figure 5. SEM images of Sn-Zn thin film (a) -1.0V/-1.3V, (b) -1.1V/-1.4V and (c) -1.2V/-1.5V

3.5. Electrochemical and electrical analyses of Sn-Zn thin films

Figure 6 shows the potentiodynamic polarization curves for the Sn-Zn thin films between -0.75 V and -0.15 V. The active polarization curves were observed for all the samples. The cathodic and anodic branches of the Tafel curves showed dramatic differences in current density for three of the samples.

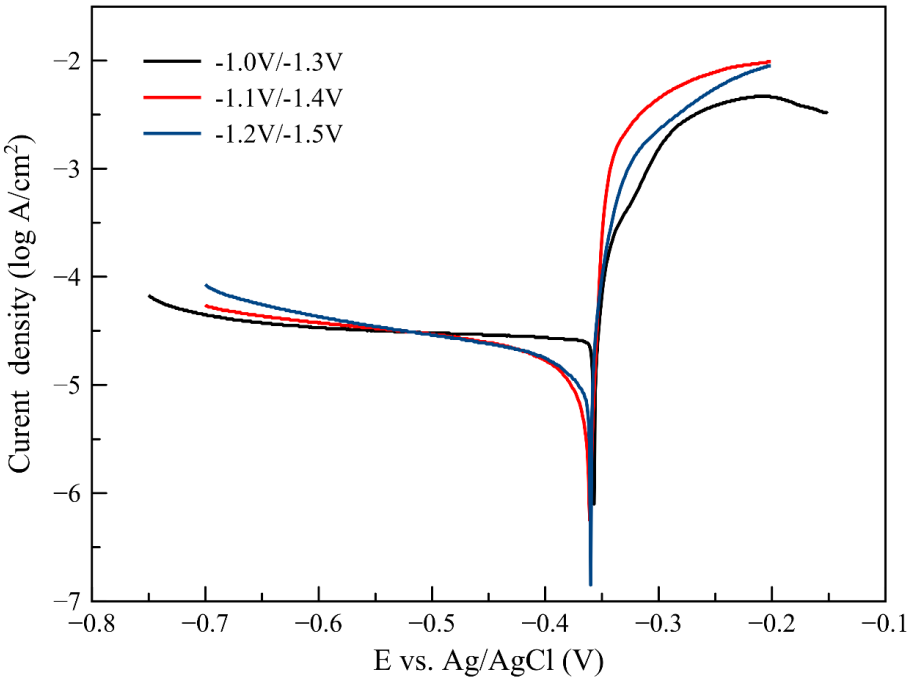

Figure 6. Potentiodynamic polarization curves of Sn-Zn thin films

Table 4 shows the potentiodynamic polarization data and the electrical resistance of the Sn-Zn thin films. The corrosion current density decreased with the increasing overpotential for the cathodic pulse potential sets. Besides that, the corrosion potential shifted to more negative potentials. The polarization resistance and the electrical resistance were increased with the increasing applied overpotential for the cathodic pulse potentials. The electrical resistance of the layers was also investigated via the four-point-probe technique and the coatings were found to be more resistant with increasing applied negative potential sets (Figure 7). The sheet resistance and specific resistance of the layers was higher than the one reported in the literature which may be due to the presence of SnO_2 and other oxides at the surface which may formed at the surface of the layer (Dybeł & Pstruś, 2023).

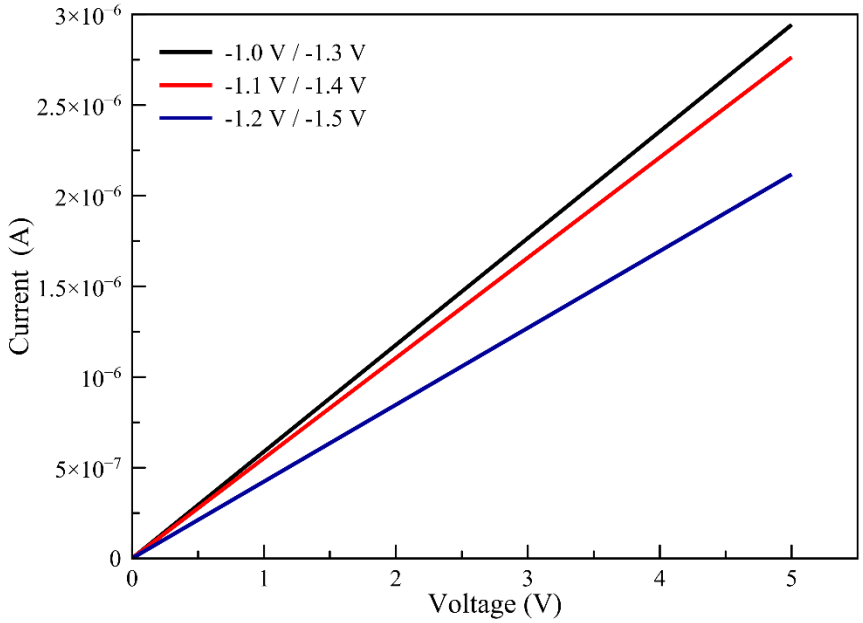

Figure 7. Current-voltage curves of the Sn-Zn thin films

In the literature, the corrosion resistance of the Sn-Zn alloys were attributed to the composition, morphology, microstructure, uniformity and the grain sizes (Benidir et al., 2022; Liu et al., 2016). It has been reported that the corrosion mechanism of the Sn-Zn thin films in NaCl solution is mainly depended on the Zn dissolution, therefore, the fine Zn grains are leading to more uniform voltage distribution over the surface, hence reducing the localized corrosion intensity and enhancing the corrosion resistance of the thin film. The corrosion resistance and the polarization resistance of Sn-Zn thin films in this study are less compared the values in the literature (Benidir et al., 2022; Liu et al., 2016). Although uniform and relatively compact layers were observed in this study, the relatively large grains led to large voltage differences over the surface and increased the corrosion current density. Besides that, the amount of Zn influences the corrosion resistance due to the electrochemical activity of Zn and the formation of ZnO and $Zn(OH)_2$ over the surface of the coating (Gerhátová et al., 2022). In the literature, the corrosion resistance of the Sn-Zn based layers was reported to be dependent on the Zn amount (Méndez et al., 2018; Mohd Nazeri et al., 2019). Also, the increasing amount of Zn was reported to increase the pitting corrosion (Mohd Nazeri et al., 2019). However, the increasing amount of possible oxide over the coating surface might influence the corrosion resistance of the relatively Zn rich layers in this layer and slightly increase the corrosion resistance compared to relatively Sn rich layers. Also, average crystal size, dislocation density and crystal density had an influence on the corrosion resistance and electrical resistivity. As the Sn phase crystal size decreased the corrosion resistance increased and as the dislocation and crystal density trend showed an increase the corrosion resistance also showed a slight increase.

According to these findings, a good corrosion resistance for Sn-Zn thin films are not only depends on the uniformity and the smooth surfaces, but also on the grain size, average crystal sizes, dislocation density and crystal density. Therefore, for future studies, cathodic pulse potential parameters can be modified to observe smaller grains and modified crystals.

Table 4. Potentiodynamic polarization data and electrical resistance of the Sn-Zn thin films

Sample	Icorr (A/cm^2)	Ecorr (mV)	Polarization Resistance ($\Omega.cm^2$)	Sheet Resistance (Ω/sq)	Specific Resistance (Ω.cm)
V/-1.3V	5.04×10^{-4}	-357	135	77×10^{-5}	2.46×10^{-5}
-1.1V/-1.4V	3.74×10^{-4}	-363	178	82×10^{-5}	3.03×10^{5}
-1.2V/-1.5V	6.44×10^{-5}	-361	190	107×10^{-5}	4.7×10^{-5}

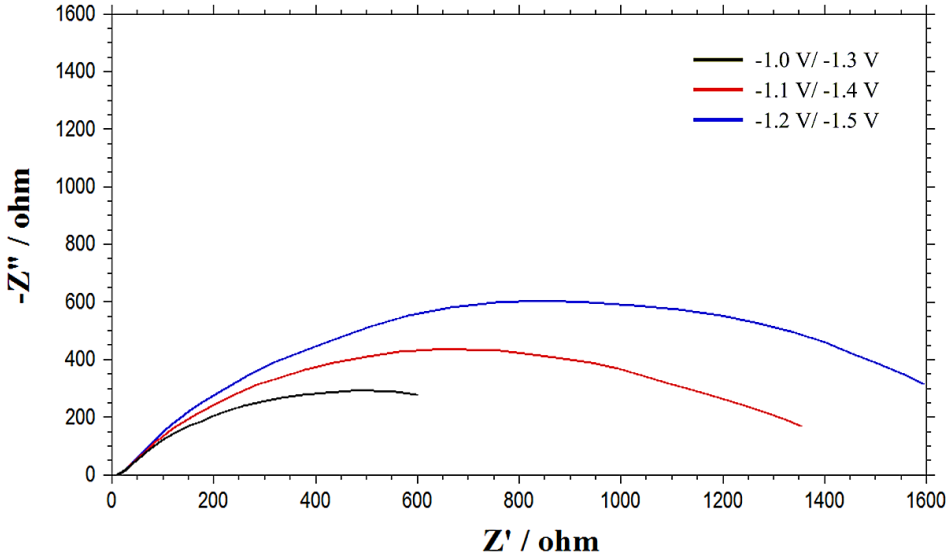

Figure 8. Nyquist curves of Sn-Zn thin films

Figure 8 shows the Nyquist plots of Sn-Zn thin films. The layers showed slightly different behavior due to the compositional and morphological changes in the layers. The curves showed the nonideal behavior of the double layer and acted like a constant phase element instead of a capacitor. As the negative applied potential set increased the curves showed relatively more capacitor-like behavior indicating an improvement in the corrosion resistance. In literature, a pseudo capacitor-like behavior was also reported for the Sn-Zn based layers with non-ideal double-layer capacitor (Méndez et al., 2018; Peng et al., 2017).

4. Conclusions

The cathodic pulse potential electrodeposition technique has been used to coat SS 316 foils with Sn-Zn thin films from a citrate-based electrolyte to minimize the harmful effects of the hydrogen evolution reaction. The potentials for the cathodic pulse potential electrodeposition were carefully selected after cyclic voltammetry studies. It has been found that relatively smooth layers with alternating compositions were coated onto the substrates with different morphologies with varying potential sets. The morphological investigations indicated that some features formed at more negative potentials than -1.4 V. The corrosion current density of the samples showed a slight increase with the increasing Zn amount and the electrical resistivity of the Sn-Zn thin films was similar. It was found that the applied overpotential and the electrodeposition mode for the potentially controlled systems can be used to modify the surface quality, morphology, and the compositional fraction of the binary coatings such as the Sn-Zn system. Designing the potentially controlled mode is particularly crucial for systems containing Zn where hydrogen evolution reaction is taking place and influencing the physical and chemical stability of the thin films. Further studies can be applied with cathodic pulse potential mode to reduce the grain size of the Sn-Zn films for enhanced corrosion resistance.

Acknowledgement

The author sincerely thanks the referees for their careful reading and valuable comments.

Author Contribution

The author contributed to all sections. The author read and approved the last version of the manuscript.

Declaration of ethical code

The author of this article declares that the material and the methods used in this study do not require ethical committee approval and/or a special legal permission.

Conflicts of interest

The author declares that she has no conflict of interest.

References

Alesary, H. F., Ismail, H. K., Shiltagh, N. M., Alattar, R. A., Ahmed, L. M., Watkins, M. J., & Ryder, K. S. (2020). Effects of additives on the electrodeposition of Zn–Sn alloys from choline chloride/ethylene glycol-based deep eutectic solvent. *Journal of Electroanalytical Chemistry*, *874*, 114517. https://doi.org/10.1016/j.jelechem.2020.114517

Baines, T., Brown, S., Benedettini, O., & Ball, P. (2012). Examining green production and its role within the competitive strategy of manufacturers. *Journal of Industrial Engineering and Management*, *5*(1), 53–87. https://doi.org/10.3926/jiem.405

Benidir, S., Madani, A., Baka, O., Kherfi, A., Delhalle, J., & Mekhalif, Z. (2022). Influence of applied potential on tin content in electrodeposition of Zn–Sn alloy coatings and its effect on corrosion protection. *Inorganic and Nano-Metal Chemistry*, *0*(0), 1–11. https://doi.org/10.1080/24701556.2021.2025105

Choi, Y. S., Ganesan, P., Kumaraguru, S. P., & Popov, B. N. (2006). Development of sacrificial Zn-Sn coatings by pulse electrodeposition process. *National Association for Surface Finishing Annual Technical Conference 2006, SUR/FIN 2006*, *1*(803), 335–350.

Dybeł, A., & Pstruś, J. (2023). New Solder Based on the Sn-Zn Eutectic with Addition of Ag, Al, and Li. *Journal of Materials Engineering and Performance*, *32*(July), 5710–5722. https://doi.org/10.1007/s11665-023-08103-0

Esfahani, M., Zhang, J., Wong, Y. C., Durandet, Y., & Wang, J. (2018). Electrodeposition of nanocrystalline zinc-tin alloy from aqueous electrolyte containing gluconate in the presence of polyethylene glycol and hexadecyltrimethylammonium bromide. *Journal of Electroanalytical Chemistry*, *813*, 143–151. https://doi.org/10.1016/j.jelechem.2018.02.021

Fashu, S., Gu, C. D., Zhang, J. L., Bai, W. Q., Wang, X. L., & Tu, J. P. (2015). Electrodeposition and characterization of Zn-Sn alloy coatings from a deep eutectic solvent based on choline chloride for corrosion protection. *Surface and Interface Analysis*, *47*(3), 403–412. https://doi.org/10.1002/sia.5728

Gerhátová, Ž., Babincová, P., Drienovský, M., Pašák, M., Černičková, I., Ďuriška, L., Havlík, R., & Palcut, M. (2022). Microstructure and Corrosion Behavior of Sn–Zn Alloys. *Materials*, *15*(20). https://doi.org/10.3390/ma15207210

Hadi Wijaya, R., & Soegijono, B. (2019). Corrosion Resistance of Sn-Zn Coated on Low Carbon Steel Material in Wet Gas Pipeline. *IOP Conference Series: Materials Science and Engineering*, *694*(1). https://doi.org/10.1088/1757-899X/694/1/012029

Hairin, A. L. N., OTHMAN, R., REZAL, F., & DAUD, F. D. M. (2018). Physiochemical Characterization of Sn-Zn Coatings Electrodeposited from an Acidic Chloride Bath in the Absence of Complexing Agent. *International Journal of Current Research in Science, Engineering & Technology*, *1*(Spl-1), 493. https://doi.org/10.30967/ijcrset.1.s1.2018.493-498

Hou, Z., Niu, T., Zhao, X., Liu, Y., & Yang, T. (2019). Intermetallic compounds formation and joints properties of electroplated Sn–Zn solder bumps with Cu substrates. *Journal of Materials Science: Materials in Electronics*, *30*(22), 20276–20284. https://doi.org/10.1007/s10854-019-02412-8

Jung, H. Y., Huang, S. Y., Ganesan, P., & Popov, B. N. (2009). Performance of gold-coated titanium bipolar plates in unitized regenerative fuel cell operation. *Journal of Power Sources*, *194*(2), 972–975. https://doi.org/10.1016/j.jpowsour.2009.06.030

Kazimierczak, H., & Ozga, P. (2013). Electrodeposition of Sn-Zn and Sn-Zn-Mo layers from citrate solutions. *Surface Science*, *607*, 33–38. https://doi.org/10.1016/j.susc.2012.08.010

Kazimierczak, H., Ozga, P., Jałowiec, A., & Kowalik, R. (2014). Tin-zinc alloy electrodeposition from aqueous citrate baths. *Surface and Coatings Technology*, *240*, 311–319. https://doi.org/10.1016/j.surfcoat.2013.12.046

Khan, S., Rasheed, M. A., Waheed, A., Shah, A., Mahmood, A., Ali, T., Nisar, A., Ahmad, M., Karim, S., & Ali, G. (2020). The role of electrodeposition current density in the synthesis and non-enzymatic glucose sensing of oxidized zinc-tin hybrid nanostructures. *Materials Science in Semiconductor Processing*, *109*(September 2019), 104953. https://doi.org/10.1016/j.mssp.2020.104953

Liu, J. C., Wang, Z. H., Xie, J. Y., Ma, J. S., Zhang, G., & Suganuma, K. (2016). Understanding corrosion mechanism of Sn-Zn alloys in NaCl solution via corrosion products characterization. *Materials and Corrosion*, *67*(5), 522–530. https://doi.org/10.1002/maco.201508605

Méndez, C. M., Scheiber, V. L., Rozicki, R. S., Kociubczyk, A. I., & Ares, A. E. (2018). Electrochemical behavior of Sn-Zn alloys with different grain structures in chloride-containing solutions. *Arabian Journal of Chemistry*, *11*(7), 1084–1096. https://doi.org/10.1016/j.arabjc.2016.12.019

Mohd Nazeri, M. F., Yahaya, M. Z., Gursel, A., Cheani, F., Masri, M. N., & Mohamad, A. A. (2019). Corrosion characterization of Sn-Zn solder: a review. *Soldering and Surface Mount Technology*, *31*(1), 52–67. https://doi.org/10.1108/SSMT-05-2018-0013

Munir, K. S., Esfahani, M., Wen, C., Zhang, J., Durandet, Y., Wang, J., & Wong, Y. C. (2018). Mechanical properties of electrodeposited nanocrystalline and ultrafine-grained Zn-Sn coatings. *Surface and Coatings Technology*, *333*(October 2017), 71–80. https://doi.org/10.1016/j.surfcoat.2017.10.059

Peng, H. T., Che, C. S., & Kong, G. (2017). Effect of minor Cu addition on corrosion behavior of Sn-Zn-xCu touch-up solder alloys. *Materials and Corrosion*, *68*(7), 791–798. https://doi.org/10.1002/maco.201609313

Pereira, J. C., dos Santos, L. P. M., Alcanfor, A. A. C., de Sant'Ana, H. B., Feitosa, F. X., Campos, O. S., Correia, A. N., Casciano, P. N. S., & de Lima-Neto, P. (2021). Effects of electrodeposition parameters on corrosion resistance of ZnSn coatings on carbon steel obtained from eutectic mixture based on choline chloride and ethylene glycol. *Journal of Alloys and Compounds*, *886*, 161159. https://doi.org/10.1016/j.jallcom.2021.161159

Pereira, Salomé, S., Pereira, C. M., & Silva, A. F. (2012). Zn-Sn electrodeposition from deep eutectic solvents containing EDTA, HEDTA, and Idranal VII. *Journal of Applied Electrochemistry*, *42*(8), 561–571. https://doi.org/10.1007/s10800-012-0431-3

Salhi, Y., Cherrouf, S., Cherkaoui, M., & Abdelouahdi, K. (2016). Electrodeposition of nanostructured Sn-Zn coatings. *Applied Surface Science*, *367*, 64–69. https://doi.org/10.1016/j.apsusc.2016.01.132

Taguchi, A. D. S., Bento, F. R., & Mascaro, L. H. (2008). Nucleation and growth of tin-zinc electrodeposits on a polycrystalline platinum electrode in tartaric acid. *Journal of the Brazilian Chemical Society*, *19*(4), 727–733. https://doi.org/10.1590/S0103-50532008000400017

Tsurusaki, T., & Ohgai, T. (2020). Mechanical properties of solder-jointed copper rods with electrodeposited Sn-Zn alloy films. *Materials*, *13*(6), 1–12. https://doi.org/10.3390/ma13061330

Yamada, M., & Usami, H. (2022). Tribological Properties of Tin-Zinc Hybrid Coating on Bronze in Lubricated Condition. *Tribology Online*, *17*(1), 54–58. https://doi.org/10.2474/trol.17.54

Zangari, G. (2015). Electrodeposition of alloys and compounds in the era of microelectronics and energy conversion technology. *Coatings*, *5*(2), 195–218. https://doi.org/10.3390/coatings5020195

Zhai, C., Zhao, D., He, Y., Huang, H., Chen, B., Wang, X., & Guo, Z. (2022). Electrolyte Additive Strategies for Suppression of Zinc Dendrites in Aqueous Zinc-Ion Batteries. *Batteries*, *8*(10). https://doi.org/10.3390/batteries8100153

Zhirnov, A. D., Karimova, S. A., Ovsyannikova, L. V., & Gubenko, O. A. (2003). New protective coatings for replacing cadmium coatings on steel parts. *Metal Science and Heat Treatment*, *45*(1–2), 23–25. https://doi.org/10.1023/A:1023939928052